Histol Histopathol (1995) 10: 673-679

Histology and Histopathology

Scanning electron and light microscopic observations on the healing process after sintered bone implantation in rats

M. Matsuda, S. Kita, M. Takekawa, S. Ohtsubo and K. Tsuyama
Department of Oral and Maxillofacial Surgery, Asahikawa Medical College, Asahikawa, Japan

Summary. The healing process after implantation of sintered bone in the rat parietal bone was compared with that of synthetic hydroxyapatite using both scanning electron and light microscopy. The results showed that the differences between the sintered natural bone and the synthetic hydroxyapatite implantations were in the states of bone union and the bioresorbability of the implanted materials, even though both materials consist of the same hydroxyapatite. In the sintered bone implantation, the newly formed bone invaded into the material at 1 to 2 weeks after implantation. The sintered bone surface on the dura mater side was completely covered by the new bone at 5 weeks. It is noteworthy that bone resorbing areas characterized by Howship's lacunae were observed on the sintered bone surface at 2 weeks and the material was replaced by new bone. Light microscopy, which revealed the invasion and the development of the new bone into the sintered bone, supported the scanning electron microscopic observations. In the synthetic hydroxyapatite, the new bone adhered closely to the material just like the sintered bone implantation. The new bone did not invade into the synthetic hydroxyapatite. There was no evidence of the resorption of the hydroxyapatite. This shows that the natural and the biological structures of the sintered bone offer an advantageous environment to fluid circulation and ingrowth after implantation.

Key words: Bone implantation, Sintered bone, Synthetic hydroxyapatite, Scanning electron microscope, Rat

Introduction

Is sintered bone useful as a material to substitute for bone?

Ueno and associates (1987) reported that sintered bone was an excellent bone substitute with biocompatibility and osteoconductive ability as compared with other bone substitutes. This material retains the bone minerals and the bone structure in its natural form, although all proteins of this material are completely removed by sintering. The surviving minerals are not only a hydroxyapatite which consists of calcium and phosphorus ions, but also some another bone minerals. The sintered bone, in addition, does not cause an immunoreaction because it has no organic components. We think that the natural bone spaces for bone marrow and blood vessels which remain after sintering provide the advantageous surroundings for the revascularization and new bone formation.

In this paper, we shall present in more detail the healing process of sintered bone implantation in comparison with that of synthetic hydroxyapatite. As a method to examine this, a scanning electron microscope as well as a conventional light microscope were used.

Offprint requests to: Prof. S. Kita, Department of Oral and Maxillofacial Surgery, Asahikawa Medical College, Asahikawa 078, Japan

Materials and methods

Preparation of implanted materials

For the sintered bone, the parietal bones from three male Fischer strain rats (aged 7 weeks, and weighing about 150 grams) were used. They were anaesthetized by an intraperitoneal injection of sodium pentobarbital (40 mg/kg) and then sacrificed by transcardial perfusion with normal saline solution. After the parietal bones were resected, peripheral soft tissue of the resected bones was removed. The resected bones were subsequently immersed in a mixture of 1% NaOH and H_2O_2 (1:1) for the removal of proteins on the bone surface (room temperature, 3 hours). The first sintering was carried out by using an electric furnace (Automatic Precision Maffle Furnace, Thomas Scientific Co., Ltd. Tokyo, Japan) at 600 ºC for 4 hours, subsequently a second sintering was performed at 1100 ºC for 3 hours with gradual cooling. The sintered bone was cut to a definite size (2x4mm) and preserved at 4 ºC.

For the control study, synthetic hydroxyapatite (APACERAM, porous and dense type, Asahi Optics INC, Tokyo, Japan) was used.

Animals

Forty male Lewis rats (aged 8 weeks) were used for the recipients in this study. They were fed conventional commercial food pellets (CE-2, Clea Japan, INC., Tokyo, Japan) and kept under optimum conditions (room temperature 22 °C; Humidity 55%; Lighting 300-500 lux; bad smell less than 20 ppm).

Twenty rats were used for the sintered bone implantation, and another twenty rats were used for the synthetic hydroxyapatite implantation. Both sintered bone and synthetic hydroxyapatite implantation were divided into four groups of 5 rats (three rats for scanning electron microscopic observation and two rats for light microscopy).

Implant procedure and tissue preparation

The rats were anaesthetized by an intraperitoneal injection of sodium pentobarbital (40 mg/Kg), and their parietal bones were exposed by ablation of the periosteum through a dermal incision. The implant site, measuring approximately 2x4 mm, was made with utmost care on the parietal bone using a dental bur mounted on a low-speed dental drill to avoid perforation of the dura mater. During bone resection, the surgical field was continuously irrigated with sterile saline solution to reduce thermal damage. The sintered bones or the synthetic hydroxyapatites were implanted in the implant site of each parietal bone, and each implanted material was finally closed by skin sutures.

At 1-3 and 5 weeks after implantation, animals of each group were anaesthetized by an intraperitoneal injection of sodium pentobarbital, and sacrificed by transcardial perfusion followed by fixation in 1.25% glutaraldehyde and 4% paraformaldehyde in 0.1 mol/l phosphate buffer (pH 7.4) for 20 minutes at room temperature. The implanted areas with peripheral host bone and soft tissue were removed.

For scanning electron microscopy, organic substances of the specimens were dissolved by 5% sodium hypochloride for 20 minutes at room temperature. They were rinsed in 0.1 mol/l phosphate buffer (pH 7.4) 3 times. They were postfixed in a 1% osmium tetroxide solution in 0.1 mol/l phosphate buffer (pH 7.4) for 90 minutes and dehydrated by a graded ethanol series. After immersion in isoamyl acetate, specimens were critical-point dried with liquid carbon dioxide, mounted on stubs, coated by gold in a vacuum device, and examined with a scanning electron microscope (S-4100, HITACHI Co., LTD, Tokyo, Japan).

For light microscopy, the specimens were rinsed in 0.05 mol/l phosphate buffer (pH 7.4) 3 times after the fixation. They were embedded in glycolmethacrylate (GMA) without decalcification, and 2 µm-thick serial sections were made. The sections were stained with haematoxylin and eosin, and observed by conventional light microscopy.

Results

Sintered bone implantation

1 week after implantation

Scanning electron microscopy showed that the sintered bone was connected to the host bone by newly-formed bone which was formed on the host bone surface of the dura mater side (Fig. 1). The newly-formed bone showed a spongy-like appearance with many vascular spaces, or the bone forming surface had osteoblastic lacunae (designated by Boyde, 1972). A part of the newly-formed bone intruded into the sintered bone (Fig. 2).

Light microscopically, the new bone was observed on the host bone surface beneath the periosteum of the dura mater side (Fig. 3). A part of the new bone lay in

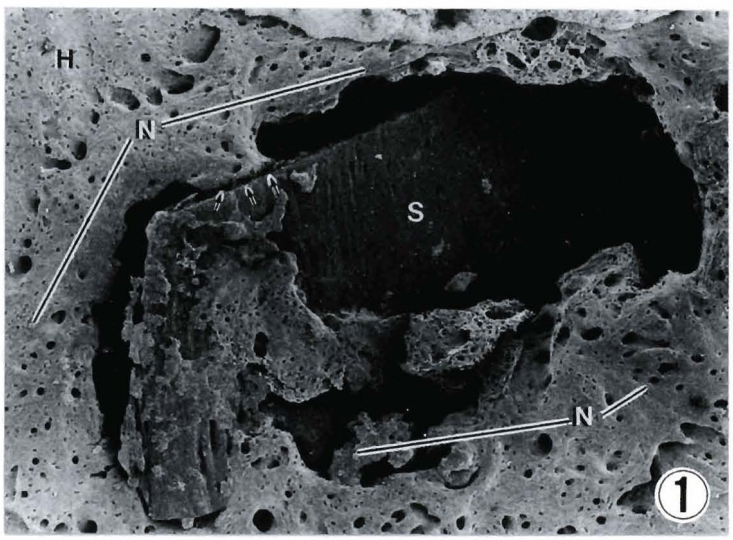

Fig. 1. Scanning electron micrograph (SEM) at 1 week after implantation of sintered bone. The new bone (N) on the host bone (H) connects to the implanted sintered bone (S). x 40

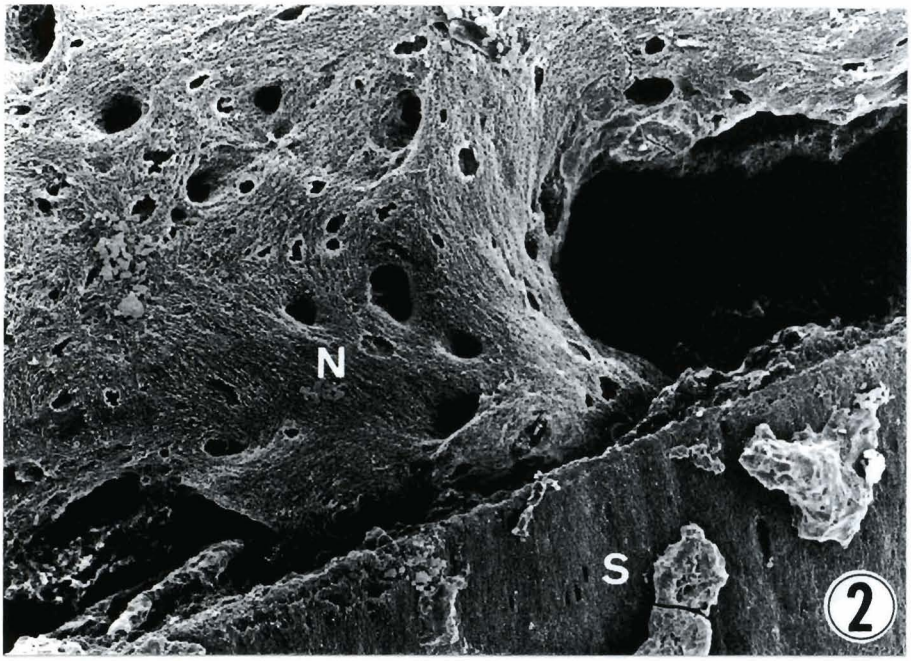

Fig. 2. High magnification of the arrows in Fig. 1. The new bone (N) intrudes into the sintered bone (S). x 200

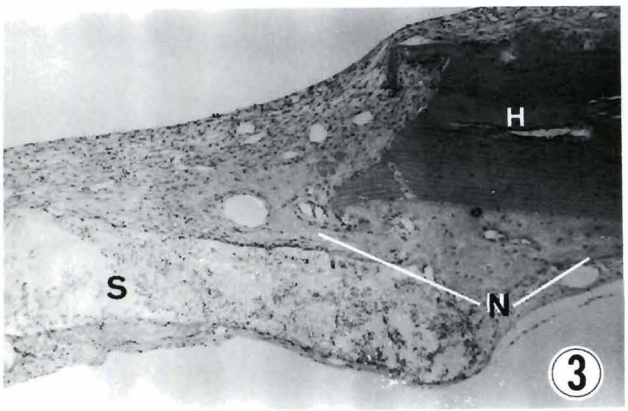

Fig. 3. Light micrograph (LM) at 1 week after implantation of the sintered bone. The upper part of the figure shows the skin side. The new bone (N) is seen on the dura mater side of the host bone (H) and contacts a part of the sintered bone (S). x 62

close contact with the sintered bone, but the greater part of the circumference of the sintered bone was enclosed by fibrous connective tissue with many blood vessels. There were no inflammatory reactions.

2 weeks after implantation

Under a scanning electron microscope, the quantity of the new bone covered on the sintered bone surface increased at the skin side, and the newly-formed bone intruded into the sintered bone (Fig. 4). Circle-like shapes surrounded by sharp edges, just like the «resorbing surface» in physiological bone described by Boyde (1972), were observed on the sintered bone surface which were located in proximity to the newly-formed bone (Fig. 5).

In light microscopic observations, the newly-formed bone came into contact with the sintered bone at the dura mater side and new bone was also seen at the inner side of the sintered bone (Fig. 6).

3 weeks after implantation

In scanning electron microscopic observation, almost all surfaces of the sintered bone in the dura mater side were covered by the newly-formed bone, although its boundary was well defined (Fig. 7). The bone union on the skin side was less marked than that of the dura mater side. The newly-formed bone became like the form of the «forming surface» (Boyde, 1972) which was characterized by numerous osteoblastic lacunae, an accumulation of spherical mineral clusters and small nodules showing a regular arrangement.

Light microscopically, the bone union by newly-formed bone from the host side was observed not only at the dura mater side but also at the skin side. The sintered bone was remarkable for its replacement of newly-formed bone in its middle parts (Fig. 8).

5 weeks after implantation

Under a scanning electron microscope, the new bone appeared to be fusing and melting into the sintered bone (Fig. 9). The demarcation line between the new bone and the sintered bone was not well defined when compared with that of 3 weeks after implantation.

Light microscopic observations were similar to those of 3 weeks after implantation.

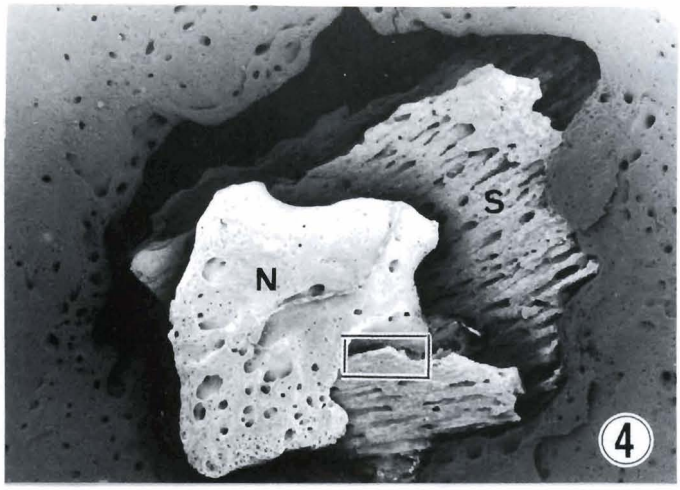

Fig. 4. SEM at 2 weeks after implantation of the sintered bone. New bone formation is seen on the skin side. The new bone (N) intrudes into the sintered bone (S). x 30

Fig. 5. High magnification of outlined area in Fig. 4. Circle-like shapes (arrows) suggesting bone resorption are seen on the sintered bone surface near the new bone (N). s= sintered bone. x 300

Fig. 6. LM at 2 weeks after implantation of the sintered bone. The upper part of the figure shows the skin side. The new bone (N) is seen at the inner side (arrow heads) of the sintered bone (S). H= host bone. x 62

Fig. 7. SEM at 3 weeks after implantation of the sintered bone. Almost all surfaces of the sintered bone (S) on the dura mater side are covered by matured new bone (N), but the boundary (arrows) between the implant and the new bone is well defined. x 30

Fig. 8. LM at 3 weeks after implantation of the sintered bone. The upper part of the figure shows the skin side. The sintered bone (S) is covered by matured new bone (N). Replacement (arrow heads) of the new bone is seen in the sintered bone. x 62

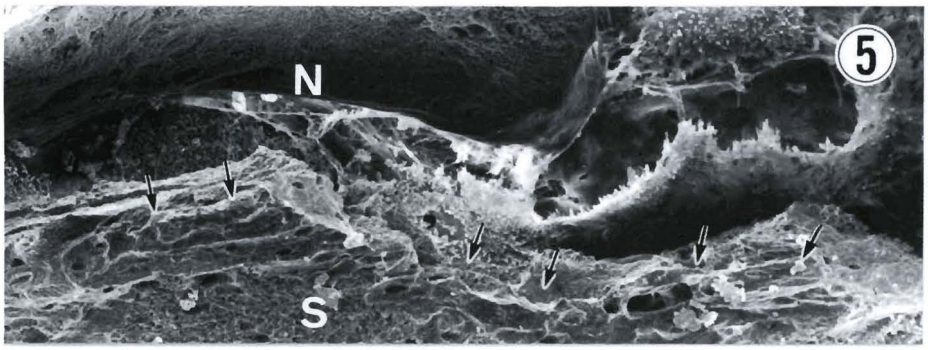

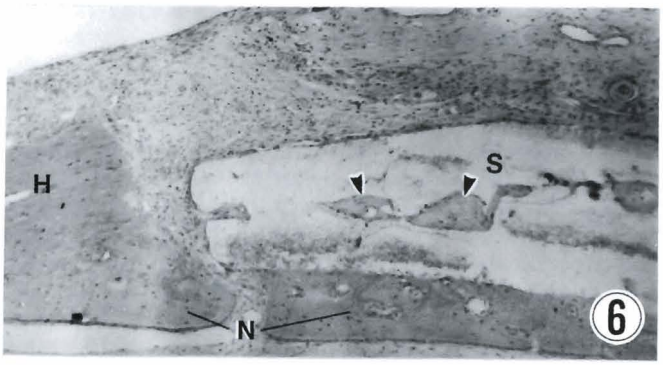

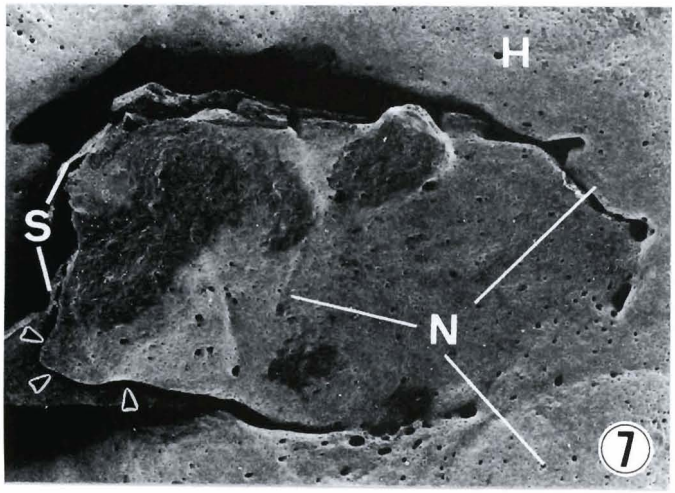

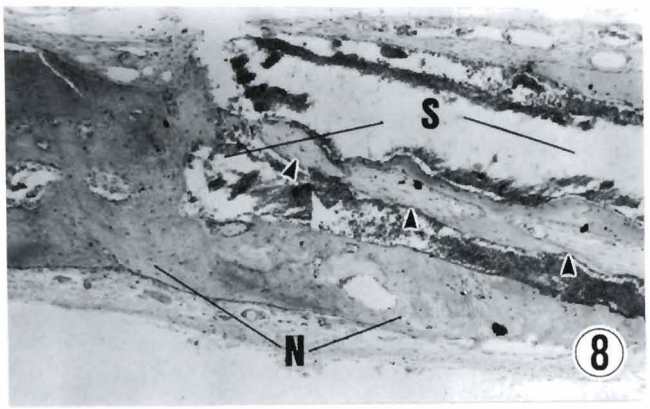

Synthetic hydroxyapatite implantation

1 week after implantation

There was no newly-formed bone on the host surface on the skin side (Fig. 10). The implanted hydroxyapatite was connected to the new bone protruding from the host bone on the dura mater side.

Light microscopically, the hydroxyapatite touched a part of the host bone, but most of the hydroxyapatite was surrounded by fibrous connective tissue. The pores of the hydroxyapatite were filled with fibrous tissue without new bone formation.

2 weeks after implantation

Scanning electron microscopy showed that new bone was formed on the host bone surface and the hydroxyapatite was surrounded by newly-formed bone on the dura mater side (Fig. 11). At the interface of the new bone and the hydroxyapatite, the new bone partially adhered to the implanted material, but most of the interface was shown as a narrow gap. On the skin side, a small amount of new bone was observed on the host bone surface.

In light microscopic observations, the new bone was formed beneath the periosteum of the host bone on the dura mater side (Fig. 12). Although the new bone developed towards the synthetic hydroxyapatite, the hydroxyapatite was still surrounded by fibrous tissues. There was no inflammatory infiltration in the fibrous tissue. The pores in the hydroxyapatite were filled with fibrous tissue with small blood vessels.

3 weeks after implantation

Under scanning electron microscope, the new bone, which was formed on host bone surface, covered the surface of the hydroxyapatite on the dura mater side, but not on all the surface (Fig. 13). A narrow gap was still seen at the interface of the new bone and the hydroxyapatite. In the pores of the hydroxyapatite, the new bone contacted the hydroxyapatite without any gaps (Fig. 14).

Light microscopically, the new bone entered into the pores of the hydroxyapatite (Fig. 15). In the pores of the inner part of the hydroxyapatite, the fibrous tissue was still observed.

5 weeks after implantation

The scanning electron microscopic and light microscopic findings of 5 weeks after implantation of the synthetic hydroxyapatite were mostly similar to those of 3 weeks after implantation.

Discussion

Our results indicate that sintered bone is a more biocompatible and osteoconductive material than synthetic hydroxyapatite. Until now histological and the transmission electron microscopic observations have shown that the synthetic hydroxyapatite was strongly connected with bone when implanted in the bone tissue and that it was a hard tissue implant material with excellent biocompatibility (Hench et al., 1971; Jarcho et al., 1977, 1978). Scanning electron and light microscopic findings of the present study show that a small gap with fibrous tissue exists in the interface between the synthetic hydroxyapatite and the new bone. In the sintered bone implantation, the new bone adheres to the sintered bone without the intervention of any fibrous tissue and it invades into the sintered bone in the early stage just after implantation. The new bone is also formed around the blood vessels of the inner part of the sintered bone, although it does not invade into the synthetic hydroxyapatite even at the five-week stage after implantation.

The sintered bone is a bone implant material which is obtained from a natural bone tissue. Therefore, it well preserves the natural three dimensional structures for the blood vessels and bone marrow (Ueno et al., 1987). The biological structure of the sintered bone, which is different from that of the synthetic hydroxyapatite, may offer an advantageous environment for fluid circulation and ingrowth after implantation.

There are some reports about the bioresorbability of the synthetic hydroxyapatite (Cameron, 1977; Klein et al., 1983; Hoogendoorn, 1984). They state that the bioresorbability of the synthetic hydroxyapatite is concerned with the temperature for crystallization, the crystallizable structure and the tricalcium phosphate (TCP) content in the hydroxyapatite. In this study, there is no evidence for the resorption of the synthetic hydroxyapatite. The scanning electron microscopic finding show the depressed areas on the sintered bone surface just like the resorbing surface in physiological bone, as described by Boyde (1972). This suggests that sintered bone might be replaced with newly-formed bone from the host bone, as well as in fresh autogenous bone transplantation. In addition to the natural bone structures of the sintered bone, Ueno et al. (1987) reported that the mineral elements of Ca, P, Na, Mg, Al, Si, Fe, Cu and Pb ions are also left in the physiological condition. Such natural conditions of the sintered bone might have an effect upon the osteoclastic bone resorption.

Many reports have shown negative views about whether or not synthetic hydroxyapatite and sintered bone have osteoinductive ability (McDavid et al., 1979; Horiuchi et al., 1988). In the present study, the new bone formation in the early stage was more dominant on the bone surface of the dura mater side than that of the skin side in both implantations. This result is strikingly similar to the results of our previous study as to the freeze-dried autogenous bone implantation and the autogenous bone transplantation which were observed by the same methods (Matsuda et al. , 1992). We believe

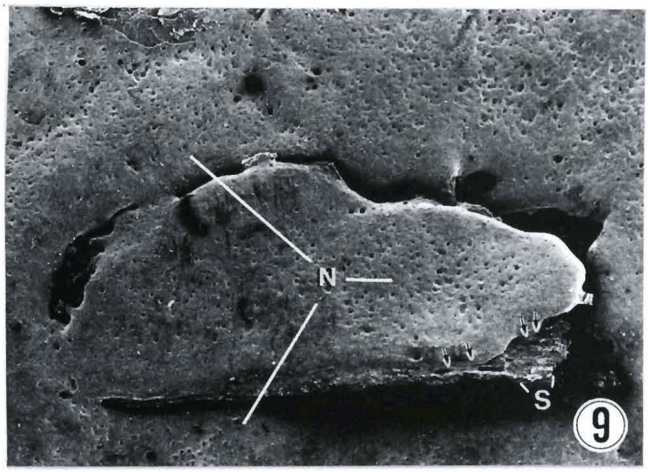
N
S
9

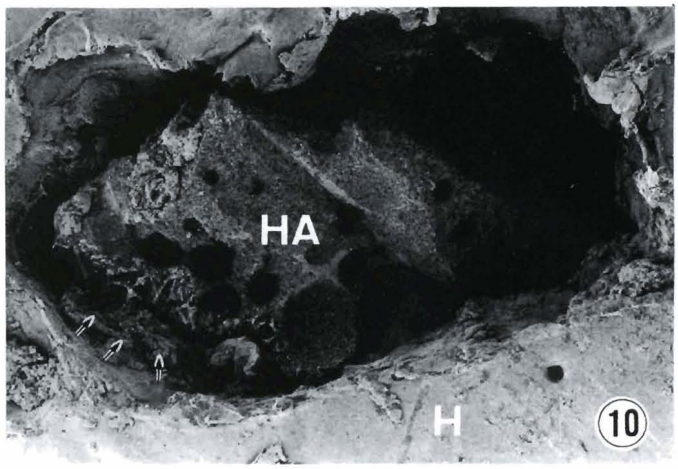
HA
H
10

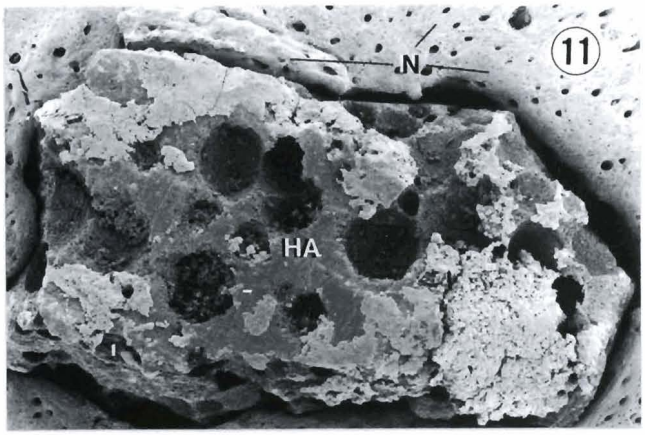
11
N
HA

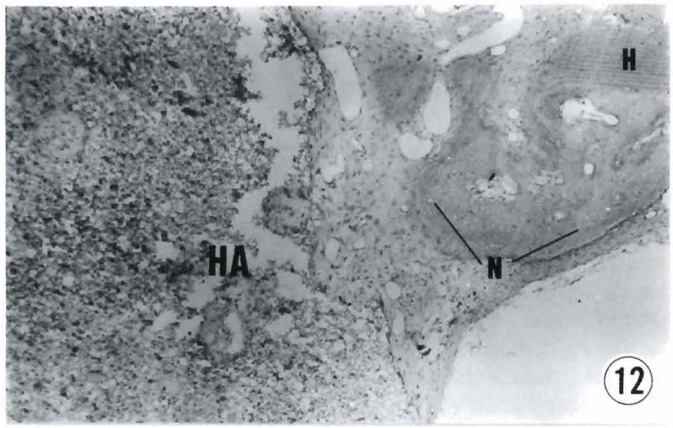
H
HA
N
12

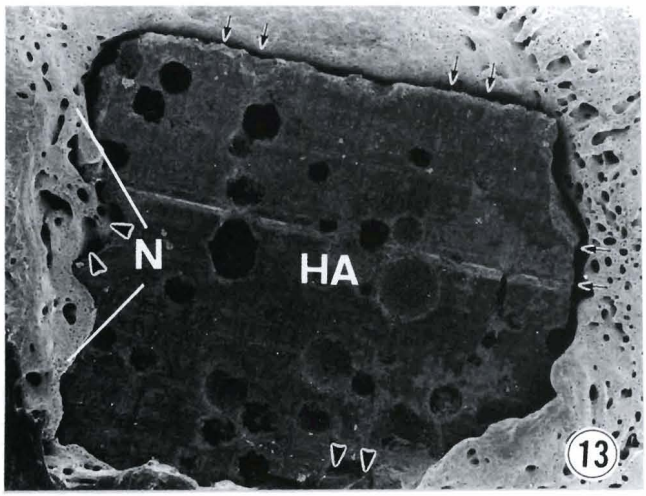
N
HA
13

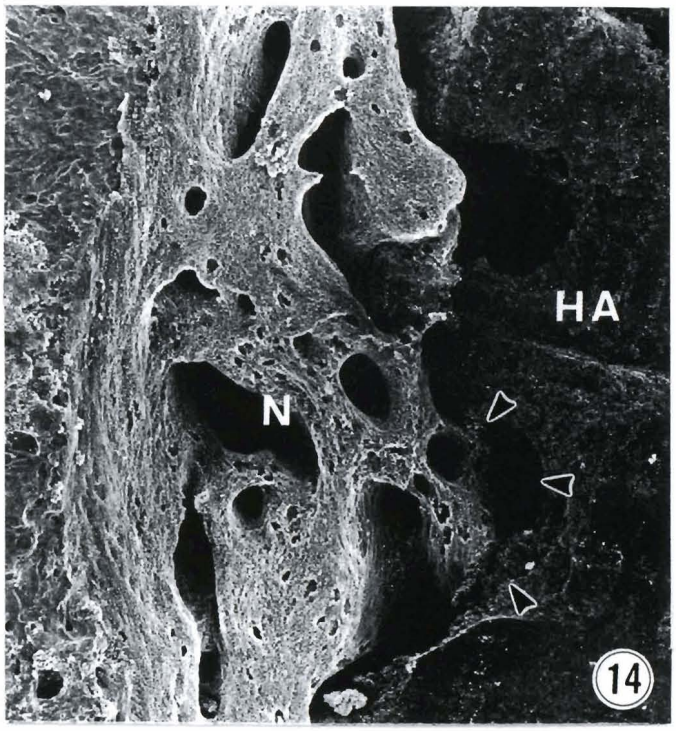
HA
N
14

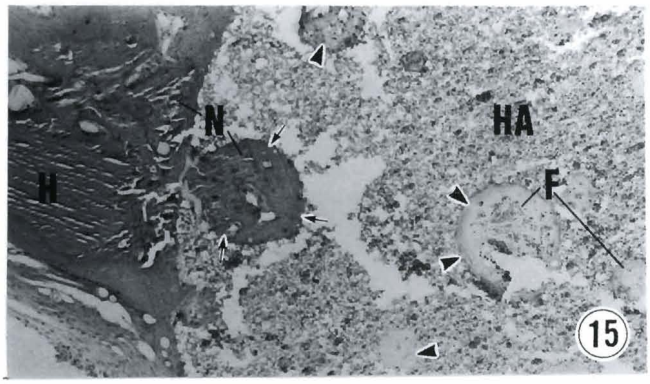
N
HA
H
F
15

Fig. 9. SEM at 5 weeks after implantation of the sintered bone. The sintered bone (S) is covered by the matured new bone (N). The demarcation line (arrows) between the implant and the new bone is not defined. x 30

Fig. 10. SEM at 1 week after implantation of the synthetic hydroxyapatite. No newly-formed bone can be seen on the host bone surface on the skin side. The new bone protruding from the dura mater side contacts the hydroxyapatite (HA). H= host bone. Arrows= contact area. x 40

Fig. 11. SEM at 2 weeks after implantation of the synthetic hydroxyapatite. The new bone (N) is formed on the host bone surface and surrounds the hydroxyapatite (HA). x 40

Fig. 12. LM at 2 weeks after implantation of synthetic hydroxyapatite. The new bone (N) develops towards the hydroxyapatite (HA), but no bone union can be seen between the new bone and the hydroxyapatite. H= host bone. x 62

Fig. 13. SEM at 3 weeks after implantation of the synthetic hydroxyapatite. The new bone (N) contacts the hydroxyapatite (HA) in the pores (arrow heads) of the hydroxyapatite. A narrow gap (arrows) can be seen in almost all of the interface of the new bone and the hydroxyapatite. x 30

Fig. 14. High magnifications of arrow-head parts in Fig. 13. The new bone (N) invades into the pores (arrow heads) of the hydroxyapatite and makes mechanical connection. HA= hydroxyapatite. x 110

Fig. 15. LM at 3 weeks after implantation of the synthetic hydroxyapatite. The new bone (N) enters into the pore of the hydroxyapatite (arrows). The pores of the inner part of the hydroxyapatite (arrow heads) are filled by fibrous tissue (F). x 62

that the origin of the newly-formed bone is the osteogenic cells which exist in the periosteum of the dura mater side which was little injured by the implant procedures. The new bone formation results from the reactive proliferation of these osteogenic cells. If the bone defect is small, it will heal up spontaneously without any implant materials. When the synthetic hydroxyapatite or the sintered bone is implanted into the bone defect, the materials are functioning as a «scaffold» for new bone formation.

In conclusion, the sintered bone turned out to be a more histocompatible and osteoconductive bone implant material than the synthetic hydroxyapatite. We suspect that the sintered bone may be replaced by newly formed bone after implantation as well as in fresh autogenous bone transplantations. The weakness of the sintered bone is its poor intensity. The improvement of the weakness without the loss of the advantages stated above will require further exploration.

Acknowledgements. The authors wish to express their thanks to Mr. K. Miyakawa for his skillful technical assistance. This work was supported by Grant No. 04671212 from the Ministry of Education of Japan.

References

Boyde A. (1972). Scanning electron microscope studies of bone. In: The biochemistry and physiology of bone. 2nd ed. Bourne G.H. (ed). Academic Press. New York. pp 259-310.

Cameron H.U. (1977). Evaluation of a biodegradable ceramic. J. Biomed. Mater. Res. 11, 179-186.

Hench L.L., Splinter R.J. and Allen W.C. (1971). Bonding mechanisms at the interface of ceramic prosthetic materials. J. Biomed. Mater. Res. Symposium. NO. 2 (part 1). pp 117-141.

Hoogendoorn H.A. (1984). Long-term study of large ceramic implants (porous hydroxyapatite) in dog femora. Clin. Orthop. 187, 281-288.

Horiuchi K., Yoshida S., Shohara E. and Sugimura M. (1988). Experimental study of xenogeneic osteogenesis using bovine sintered bone true bone ceramic (TBC) combined with bovine bone morphogeneic protein (bBMP). Deut. Zahnärztl. Z. 43, 93-96.

Jarcho M., Kay J.F., Gumaer K.I., Doremus R.H. and Drobeck H.P. (1977). Tissue, cellular and subcellular events at a bone-ceramic hydroxyapatite interface. J. Bioengin. 1, 79-92.

Jarcho M., Jatsy V., Gumaer K.I., Kay J.F. and Doremus R.H. (1978). Electron microscopic study of a bone-hydroxyapatite implant interface. Trans. 4th Ann. Met. Soc. Biomater. 10th Int. Biomater. Symp. p 112.

Klein C.P.A.T., Driessen A.A., de-Groot K. and van den Hooff A. (1983). Biodegradation behavior of various calcium phosphate materials in bone tissue. J. Biomed. Mater. Res. 17, 769-784.

Matsuda M., Satoh Y. and Ono K. (1992). Scanning electron microscopic and light microscopic observation on morphological changes of freeze-dried bone implantation in rats: Comparison with fresh autogenous bone transplantation. Histol. Histopathol. 7, 393-403.

McDavid P.T., Boone M.E. 2d., Kafrawy A.H. and Mitchell D.F. (1979). Effect of autogenous marrow and calcitonin on reactions to a ceramic. J. Dent. Res. 58, 1478-1483.

Ueno Y., Shima Y. and Akiyama T. (1987). Development of new biomaterial as a bone substitute; true bone ceramics. In: Materials Science Monographs, 39. Ceramics in Clinical applications. Vincentini P. (ed). Proceedings of the International Symposium on Bioceramics. 369-378.

Accepted March 10, 1995